Application of the detailed balance model to thermoradiative cells based on a p-type two-dimensional indium selenide semiconductor

Muhammad Yusrul Hanna[1,2*], Ahmad R. T. Nugraha[2], Muhammad Aziz Majidi[1]
[1]Department of Physics, Faculty of Mathematics and Natural Sciences, Universitas Indonesia, Indonesia
[2]Research Center for Physics, National Research and Innovation Agency (BRIN), Indonesia

Abstract
Thermoradiative (TR) cells are energy conversion devices that convert low-temperature waste heat to electricity. TR cells work on the same principles as photovoltaics, but they produce a reverse bias voltage due to higher cell temperature than the environment temperature. Depending on the energy gap of the material, temperature difference would generate electrical energy by electron-hole pair recombination. In this work, we propose a two-dimensional (2D) InSe for applications in the TR cells. The electronic properties of 2D InSe are obtained by using first-principles calculations. Then, the calculated energy gap is used to estimate output power density and efficiency according to the Shockley-Queisser framework through a detailed balance model adapted with the TR cells. Using a heat source at T_c = 1000 K and the ambient temperature T_a = 300 K, an ideal TR cell of 2D InSe at the maximum power point can achieve output power density and efficiency up to 0.061 W/m^2 and 4.41%, respectively, with an energy gap of 1.43 eV. However, sub-bandgap and non-radiative losses will degenerate the cell's performance significantly.

INTRODUCTION

Currently, the search for renewable energy has become increasingly significant for the scientific community. However, environmental pollution generated by gas emissions from the combustion of fossil fuels has also contributed to global warming. Therefore, the quest for clean energy needs to be encouraged, such as solar energy harvesting. Conventional photovoltaics, one of the solar harvesting energy systems, can generate electricity throughout daytime hours; however, it is not perfect for the nighttime [1]. Therefore, a new system is needed to generate electricity at night. In this case, thermoradiative (TR) cells may play an essential role [1-15].

The (TR) cells operate similarly to the photovoltaic (PV) cells; they generate energy by transferring radiative heat between two reservoirs with varying temperatures [1, 3-15]. The fundamental difference is that the PV cells generate the electric current kept at low temperatures. In contrast, the TR cells are kept at high temperatures to generate electric current [1, 7, 10, 11]. As a result, the photon flux absorbed is less than the photon flux emitted, giving an electron-hole pair population (np) below the thermal equilibrium (n_i^2) and delivering power when operated with a reverse bias across the junction [1, 4, 5, 6, 10].

The TR cells in their simplest form consist of a p-n junction that allows electron-hole pair recombination throughout the bandgap. Theoretically, the bandgap is essential in increasing the maximum efficiency for the TR cells according to the detailed balance model [10]. Consequently, materials with a tunable bandgap can enhance the cell's power. Some examples of

such materials are transition metal dichalcogenides (TMD), black phosphorous (BP), and group III chalcogenides in the family of two-dimensional (2D) semiconductors [16][17]. In particular, the band structure of monolayer group III chalcogenides is quite unusual, consisting of a parabolic band at the conduction band maximum (CBM) and a flat band at the valence band minimum (VBM). As a result, a sharp peak emerges in the density of states (DOS) at the VBM and is almost constant at the CBM [18][19].

Among monolayer group III chalcogenides, indium selenide (InSe) has attracted much attention, especially for thermoelectric applications [20] because the thermal conductivity of InSe is lower than other monolayer group-III chalcogenides (such as GaSe and GaS) [21]. From the previous work, the maximum power factor of monolayer InSe can be obtained at T = 300 K in the armchair direction for the p-type doping [20], where the power factor is defined by $S^2 \sigma$ (S and σ are Seebeck coefficient and electrical conductivity, respectively). In this work, we propose that the p-type monolayer InSe is also potentially useful for the TR cells. To determine the efficiency of the TR cells beyond their upper limit, we require an energy gap from the electronic structure. The first-principles density-functional theory (DFT) calculation allows for the electronic structure computation. Then, the energy gap is used to determine the power conversion efficiency using the Shockley-Queisser framework through the detailed balance model adapted to the TR cells [10][22].

METHOD

We perform the DFT calculation implemented in the Quantum ESPRESSO package [23] to obtain structural optimization and electronic properties. We employ the generalized gradient approximation (GGA) [24] without spin-orbit coupling to consider the exchange-correlation functional, while the pseudopotentials are chosen to be norm-conserving [25][26]. The GGA with spin-orbit coupling and Coulomb repulsion U is unnecessary in the calculation because InSe is not a strongly-correlated material [18, 19, 20, 27].

The wave function is defined by the plane-wave basis set with a kinetic energy cutoff of 60 Ry. We employ 16×16×1 Monkhorst-Pack k-mesh to sample Brillouin zone integration. The optimized tetrahedron method [28] is used to calculate the DOS, defined as the number of states at a given energy. The system is modelled using a hexagonal lattice with a space group P-6m2 (187). The vacuum distance is set to 25 Å to avoid interaction between adjacent layers, as shown in Figure 1.

Having information about the energy gap of materials, we can calculate the TR cells' power density and efficiency. Using the detailed balance model (DBM) of TR cells, Strandberg [10] assumed that the energy discrepancy among the quasi-Fermi levels of the electron and hole is equivalent to the energy gap of the semiconductor. In the TR cells, the net absorption of photons equals the number of electrons produced by the cell to an external circuit. Therefore, the current density is given by

$$J = q\left[\dot{N}(T_a, 0) - \dot{N}(T_c, \Delta\mu_c)\right], \qquad (1)$$

where T_a, T_c, and q are the ambient temperature, the cell temperature, and the elementary charge, respectively. In equation (1), $\Delta\mu_c$ is the energy difference among the quasi-Fermi level of the electron and the holes, assumed constant with the energy gap. $\dot{N}(T_a, 0)$ represents the flux of photons absorbed from the environment, whereas $\dot{N}(T_c, \Delta\mu_c)$ represents the flux of photons emitted into the environment. The photon flux emitted by the cell can be calculated using the formula below [29]
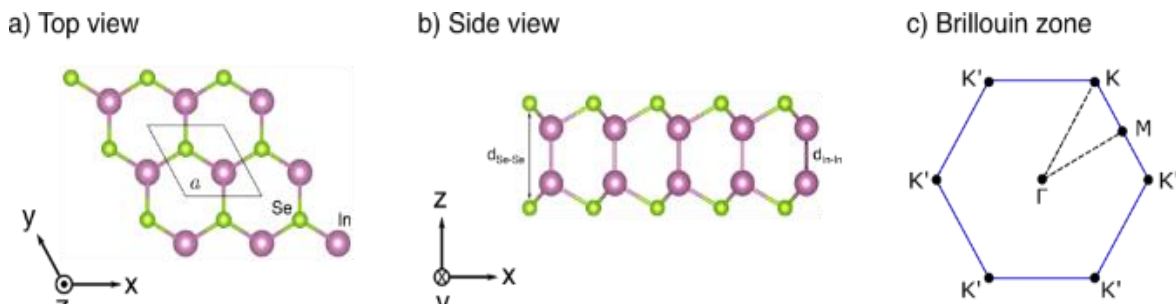

Figure 1. Geometric structure of monolayer InSe, (a) top view, (b) side view of the unit cell, and (c) Brillouin zone in reciprocal lattice. There are two sublayers in a monolayer InSe. The x- and y- axes represent the armchair and zigzag directions, respectively

$$\dot{N}(T, \Delta\mu) = \frac{2\pi}{h^3 c^2} \int_{E_g}^{\infty} \frac{E^2}{\exp\left(\frac{E - \Delta\mu}{kT}\right) - 1} dE, \quad (2)$$

where h is the Planck constant, c is the speed of light in a vacuum, k is Boltzmann's constant, T is the temperature, and $\Delta\mu$ is the chemical potential to drive emission. The voltage V within the cell's two contacts is well known in semiconductor physics to be given by $V = \Delta\mu/q$ so that the power density can be written as

$$P = JV = qV[\dot{N}(T_a, 0) - \dot{N}(T_c, \Delta\mu_c)]. \quad (3)$$

The efficiency η of the TR cells is expressed as the ratio of the output electric power to the supplied heat, i.e.,

$$\eta = \frac{P}{Q_{in}} = \frac{P}{P + \dot{E}_{rad} - \dot{E}_{abs}}, \quad (4)$$

where $\dot{E}_{abs} = \dot{E}_{ph}(T_a, 0)$ is the cell's absorbed radiative energy flux and $\dot{E}_{rad} = \dot{E}_{ph}(T_c, \Delta\mu_c)$ is the cell's radiative energy flux given by

$$\dot{E}(T, \Delta\mu) = \frac{2\pi}{h^3 c^2} \int_{E_g}^{\infty} \frac{E^3}{\exp\left(\frac{E - \Delta\mu}{kT}\right) - 1} dE. \quad (5)$$

RESULTS AND DISCUSSION

From the calculation of optimized geometry, we obtain that the lattice constant of monolayer InSe is 4.078 Å. The monolayer InSe has two sublayers, with the first and second sublayers separated by d_{In-In} =2.826 Å and d_{Se-Se}= 5.387 Å, as shown in Figure 1. Figure 2(a) shows the calculated band structure for monolayer InSe using GGA-PBE calculation. Our DFT calculation parameters show that the monolayer InSe exhibits an indirect bandgap of about 1.43 eV, consistent with the previous study [18, 19, 20, 27]. The CBM appears at the Γ-point, while the VBM is at a point along the $K - \Gamma$ direction. In this case, we set E_F = 0. Figure 2(b) illustrates a very sharp DOS at the valence band's top. In the conduction band, a finite and nearly constant 2D DOS emerges.

Using the result from the DFT calculation, we use the bandgap E_g = 1.43 eV to simulate the thermoradiative properties of monolayer InSe. In all of the following calculations, the environment is set at T_a = 300 K and three different heat sources are considered at T_c = 500, 750, and 1000 K. Figure 3 shows the J-V curves at different heat source temperatures.
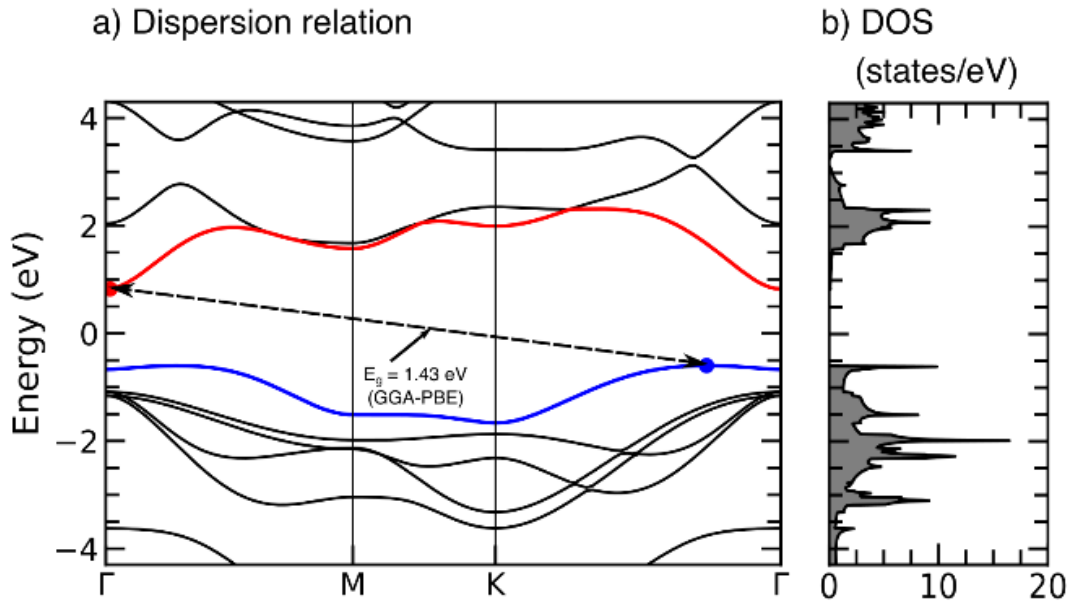

Figure 2. Electronic structure of monolayer InSe. (a) Energy dispersion relation along the path of high symmetry points Γ-M-K-Γ. (b) Density-of-states (DOS).
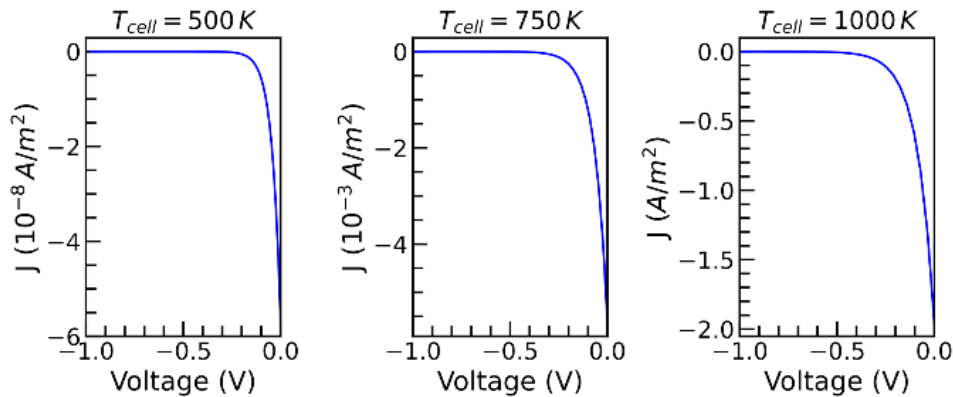
Figure 3. J-V curves of a TR cell with an energy gap of 1.43 eV. The environment temperature is T_a = 300 K, while the heat source temperature is T_c = 500, 750, and 1000 K.

Each heat source temperature (T_c) and the environment temperature (T_a) will contribute to an open-circuit voltage (V_{oc}). The open-circuit voltage is a condition where the net current is zero. The open-circuit voltage in this TR cell has a negative value because the photon flux absorbed is less than the photon flux emitted.

Figures 4 and Figure 5 respectively depict the output power density and the efficiency of a monolayer InSe. For T_c = 500 K, the TR cell only produces a minimal output power (maximum power point or MPP = 9.0248×10^{-10} W/m^2).
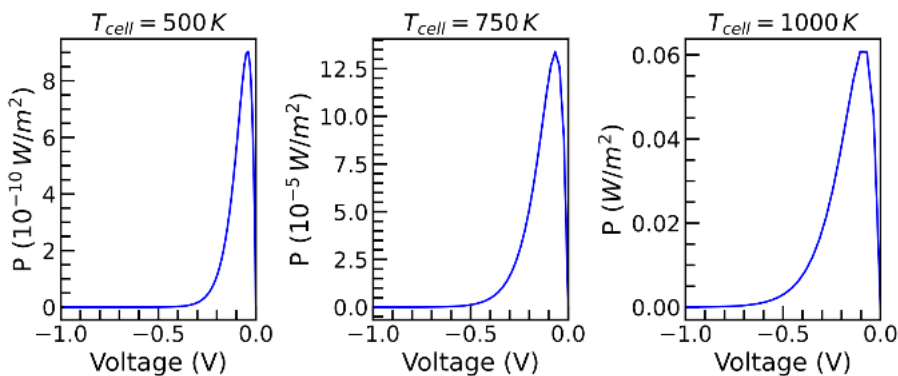

Figure 4. The output power density for a TR cell as a function of cell voltage for heat source temperatures (T_c = 500, 750, and 1000 K) and environment temperature T_a= 300 K)
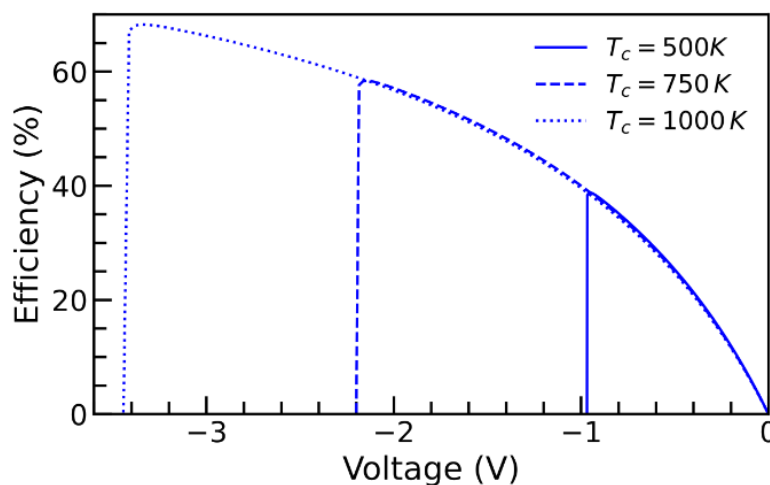

Figure 5. The efficiency for a TR cell as a function of cell voltage for heat source temperatures (T_c = 500, 750, and 1000 K) and the environment temperature (T_a= 300 K).

On the other hand, when the TR cell is working at T_c = 1000 K, we obtain MPP = 0.06 W/m^2. At the MPP, an ideal cell with an energy gap of 1.43 eV has an efficiency of 4.41% with delivering output power of 0.06 W/m^2 at T_c= 1000 K. According to Figure 4 and Figure 5, the MPP increases with the temperature. Consequently, when the material has an energy gap larger than kT, the maximum efficiency approaches the Carnot efficiency ($\eta_{Carnot} = 1 - T_a/T_c$) [10]. Therefore, both power density and conversion efficiency also increase with the temperature. Note that the TR cell within this work does not possess a critical temperature for efficiency, but only the bandgap of the material determines the upper limit of the efficiency.

CONCLUSION

We have conducted a theoretical investigation on a TR cell using monolayer InSe as an emissive energy harvester. The detailed balance model determined the optimized geometry and electronic structures using DFT calculations to estimate the bandgap and the TR cell's power conversion efficiency. With a heat source set to T_c = 1000 K and an ambient temperature of T_a = 300 K, an ideal TR cell of 2D InSe can achieve MPP and MEP values of up to 0.0607 W/m^2 and 4.41%, respectively, with a 1.43 eV energy gap. Both power density and conversion efficiency can be improved by increasing the cell temperature. It should be noted that suppression of non-radiative processes such as spin-orbit interaction, Auger process, Shockley-Read-Hall recombination, and surface defect scattering in the nonmagnetic material will give some opportunity to enhance the efficiency of TR cells. The upper limit of TR cell efficiency, in this case, will follow the detailed balance model representation.

ACKNOWLEDGMENT

REFERENCES

[1] T. Deppe and J. N. Munday, "Nighttime Photovoltaic Cells: Electrical Power Generation by Optically Coupling with Deep Space," *ACS Photonics,* vol. 7, p. 1–9, 2020, doi: 10.1021/acsphotonics.9b00679.

[2] S. V. Boriskina, J. K. Tong, W.-C. Hsu, B. Liao, Y. Huang, V. Chiloyan and G. Chen, "Heat meets light on the nanoscale," *Nanophotonics,* vol. 5, p. 134–160, 2016, doi: 10.1515/nanoph-2016-0010.

[3] J. J. Fernández, "Thermoradiative Energy Conversion With Quasi-Fermi Level Variations," *in IEEE Transactions on Electron Devices,* vol. 64, no. 1, pp. 250-255, Jan. 2017, doi: 10.1109/TED.2016.2627605.

[4] G. García, J. J. Fernández, P. Palacios and P. Wahnón, "Thermoradiative Cells Based on a p-type Cu3SbSe4 Semiconductor: Application of a Detailed Balance Model," *Journal of Electronic Materials,* vol. 48, pp. 6777-6785, 2019, doi: 10.1007/s11664-019-07485-z.

[5] W.-C. Hsu, J. K. Tong, B. Liao, Y. Huang, S. V. Boriskina and G. Chen, "Entropic and Near-Field Improvements of Thermoradiative Cells," *Scientific Reports,* vol. 6, pp. 34837, 2016, doi: 10.1038/srep34837.

[6] T. Liao, X. Zhang, X. Chen, B. Lin and J. Chen, "Negative illumination thermoradiative solar cell," *Optics Letters,* vol. 42, no. 16, pp. 3236–3238, 2017, doi: 10.1364/OL.42.003236.

[7] C. Lin, B. Wang, K. H. Teo and Z. Zhang, "Near-field enhancement of thermoradiative devices," *AIP Journal of Applied Physics.,* vol. 122, pp. 143102, 2017, doi: 10.1063/1.5007036.

[8] A. Pusch, J. M. Gordon, A. Mellor, J. J. Krich and N. J. Ekins-Daukes, "Fundamental Efficiency Bounds for the Conversion of a Radiative Heat Engine's Own Emission into Work," *Physical Review Applied,* vol. 12, no. 6, pp. 064018, 2019.

[9] P. Santhanam and S. Fan, "Thermal-to-electrical energy conversion by diodes under negative illumination," *Physical Review B,* vol. 93, no. 16, p. 161410, 2016.

[10] R. Strandberg, "Theoretical efficiency limits for thermoradiative energy conversion," *Journal of Applied Physics,* vol. 117, no. 5, pp. 055105, 2015, doi: 10.1063/1.4907392.

[11] E. J. Tervo, W. A. Callahan, E. S. Toberer, M. A. Steiner and A. J. Ferguson, "Solar Thermoradiative-Photovoltaic Energy Conversion," *Cell Reports Physical Science,* vol. 1, no. 12, pp. 100258, 2020, doi: 10.1016/j.xcrp.2020.100258.

[12] Z. Ye, W. Peng, S. Su and J. Chen, "Intermediate Band Thermoradiative Cells," in *IEEE Transactions on Electron Devices,* vol. 65, no. 12, pp. 5428-5433, Dec. 2018, doi: 10.1109/TED.2018.2873581.

[13] X. Zhang, Y. S. Ang, J. can Chen and L. K. Ang, "Design of an InSb thermoradiative system for harvesting low-grade waste heat," *Optics Letters,* vol. 44, no. 13, pp. 3354-3357, 2019, doi: 10.1364/OL.44.003354.

[14] X. Zhang, J. Du, J. Chen, L. K. Ang and Y. S. Ang, "Designing high-performance nighttime thermoradiative systems for harvesting energy from outer space," *Optics Letters,* vol. 45, no. 21, pp. 5929–5932, 2020, doi: 10.1364/OL.400349.

[15] X. Zhang, W. Peng, J. Lin, X. Chen and J. Chen, "Parametric design criteria of an updated thermoradiative cell operating at optimal states," *Journal of Applied Physics,* vol. 122, no. 17, pp. 174505, 2017, doi: 10.1063/1.4998002.

[16] N. T. Hung, E. H. Hasdeo, A. R. T. Nugraha, M. S. Dresselhaus and R. Saito, "Quantum Effects in the Thermoelectric Power Factor of Low-Dimensional Semiconductors," *Physical Review Letter,* vol. 117, pp. 036602, 2016.

[17] Y. Saito, T. Iizuka, T. Koretsune, R. Arita, S. Shimizu and Y. Iwasa, "Gate-Tuned Thermoelectric Power in Black Phosphorus," *Nano Lett.,* vol. 16, no. 8, pp. 4819-4824, 2016, doi: 0.1021/acs.nanolett.6b00999.

[18] V. Zólyomi, N. D. Drummond and V. I. Fal'ko, "Band structure and optical transitions in atomic layers of hexagonal gallium chalcogenides," *Physical Review B,* vol. 87, no. 19, p. 195403, 2013.

[19] V. Zólyomi, N. D. Drummond and V. I. Fal'ko, "Electrons and phonons in single layers of hexagonal indium chalcogenides from ab initio calculations," *Physical Review B,* vol. 89, no. 20, pp. 205416, 2014.

[20] N. T. Hung, A. R. T. Nugraha and R. Saito, "Two-dimensional InSe as a potential thermoelectric material," *AIP Applied Physics Letters,* vol. 111, no. 9, pp. 092107, 2017, doi: 10.1063/1.5001184.

[21] T. Pandey, D. S. Parker and L. Lindsay, "Ab initio phonon thermal transport in monolayer InSe, GaSe, GaS, and alloys," *Nanotechnology,* vol. 28, no. 45, pp. 455706, 2017.

[22] W. Shockley and H. J. Queisser, "Detailed Balance Limit of Efficiency of p-n Junction Solar Cells," *J. Appl. Phys.,* vol. 32, pp. 510-519, 1961.

[23] P. Giannozzi et al., , "Advanced capabilities for materials modelling with QUANTUM ESPRESSO," *J. Phys. Condens. Matter,* vol. 29, p. 465901, 2017.

[24] J. P. Perdew, K. Burke and M. Ernzerhof, "Generalized Gradient Approximation Made Simple," *Phys. Rev. Lett.,* vol. 77, no. 18, p. 3865–3868, 1996, doi: 10.1103/ PhysRevLett.77.3865

[25] D. R. Hamann, M. Schlüter and C. Chiang, "Norm-Conserving Pseudopotentials," *Phys. Rev. Lett.,* vol. 43, no. 20, p. 1494–1497, 11 1979.

[26] G. B. Bachelet, D. R. Hamann and M. Schlüter, "Pseudopotentials that work: From H to Pu," *Phys. Rev. B,* vol. 26, no. 8, p. 4199–4228, 10 1982.

[27] L. Debbichi, O. Eriksson and S. Lebègue, "Two-Dimensional Indium Selenides Compounds: An Ab Initio Study," *J. Phys. Chem. Lett.,* vol. 6, no. 15, pp. 3098-3103, 2015, doi: 10.1021/acs.jpclett.5b01356

[28] M. Kawamura, Y. Gohda and S. Tsuneyuki, "Improved tetrahedron method for the Brillouin-zone integration applicable to response functions," *Physical Review B,* vol. 89, no. 9, p. 094515, 2014, doi: 10.1103/PhysRevB.89.094515.

[29] A. De Vos and H. Pauwels, "On the thermodynamic limit of photovoltaic energy conversion," *Applied physics,* vol. 25, pp. 119-125, 1981, doi: 10.1007/BF00901283.